

## Rotaxanes

# Ring-to-Thread Chirality Transfer in [2]Rotaxanes for the Synthesis of Enantioenriched Lactams

Carmen Lopez-Leonardo, Adrian Saura-Sanmartin, Marta Marin-Luna, Mateo Alajarin, Alberto Martinez-Cuezva,\* and Jose Berna\*

**Abstract:** The synthesis of chiral mechanically interlocked molecules has attracted a lot of attention in the last few years, with applications in different fields, such as asymmetric catalysis or sensing. Herein we describe the synthesis of orientational mechanostereoisomers, which include a benzylic amide macrocycle with a stereogenic center, and nonsymmetric *N*-(arylmethyl)fumaramides as the axis. The base-promoted cyclization of the initial fumaramide thread allows enantioenriched value-added compounds, such as lactams of different ring sizes and amino acids, to be obtained. The chiral information is effectively transmitted across the mechanical bond from the encircling ring to the interlocked lactam. High levels of enantioselectivity and full control of the regioselectivity of the final cyclic compounds are attained.

## Introduction

The synthesis of chiral organic molecules is the focus of countless efforts of the scientific community because of their significance in key global industries, such as pharmaceuticals or cosmetics.<sup>[1]</sup> In most organic molecules, the chiral information is incorporated through stereogenic carbon atoms, although other less conventional stereogenic units can also be integrated to induce asymmetry, such as helical or planar chiral elements.<sup>[2]</sup>

In parallel, the synthesis of enantioenriched mechanically interlocked molecules has importantly evolved in the last years,<sup>[3,4]</sup> finding exciting applications in the field of asymmetric catalysis<sup>[5]</sup> or sensing of chiral molecules.<sup>[6,7]</sup> The

structure of the mechanically interlocked molecules (MIMs),<sup>[8]</sup> with at least two components, increases the number of possibilities for the introduction of chirality, incorporating stereogenic units (including point or axial elements), either on the macrocycles or threads in [2]rotaxanes.<sup>[4]</sup>

Additionally, MIMs can exhibit other stereogenic elements which arise as a consequence of the mechanical bond, highlighting the co-conformational point chirality<sup>[9]</sup> or the mechanically planar chirality.<sup>[10–13]</sup> Thus, a mechanically planar chiral rotaxane can be prepared by a combination of a  $C_{nh}$  macrocycle that surrounds a  $C_{nv}$  thread, being both components achiral (Figure 1A). The mechanical bond precludes the rotational symmetry of the components, being possible to distinguish two mechanically planar enantiomers. Because of the surge of mechanical chirality in the starting [2]rotaxanes we have used as starting materials in this work, another type of chiral MIMs requires a special comment: the orientational mechanostereoisomers (Figure 1B). The orientational mechanostereoisomers contains a macrocycle having stereogenic centers in its backbone. These types of rings

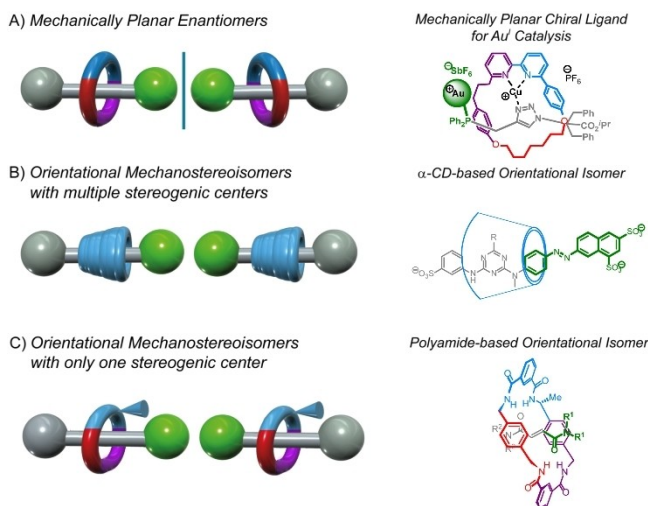


**Figure 1.** Schematic representations of: A) a pair of mechanically planar rotaxanes (*enantiomers*) and one example of a mechanically planar ligand used in Au<sup>I</sup> catalysis,<sup>[11]</sup> B) two orientational mechanostereoisomers and an example of a  $\alpha$ -CD-based orientational isomer having multiple stereocenters at the ring;<sup>[15]</sup> C) orientational mechanostereoisomers with a single stereogenic center, and a general representation of an isomer having just one stereogenic center at the ring (*this work*).

[\*] Dr. C. Lopez-Leonardo, Dr. A. Saura-Sanmartin, Dr. M. Marin-Luna, Prof. M. Alajarin, Dr. A. Martinez-Cuezva, Dr. J. Berna  
 Departamento de Química Orgánica, Facultad de Química, Regional Campus of International Excellence “Campus Mare Nostrum”,  
 Universidad de Murcia  
 30100 Murcia (Spain)  
 E-mail: amcuezva@um.es  
 ppberna@um.es

© 2022 The Authors. Angewandte Chemie International Edition published by Wiley-VCH GmbH. This is an open access article under the terms of the Creative Commons Attribution Non-Commercial License, which permits use, distribution and reproduction in any medium, provided the original work is properly cited and is not used for commercial purposes.

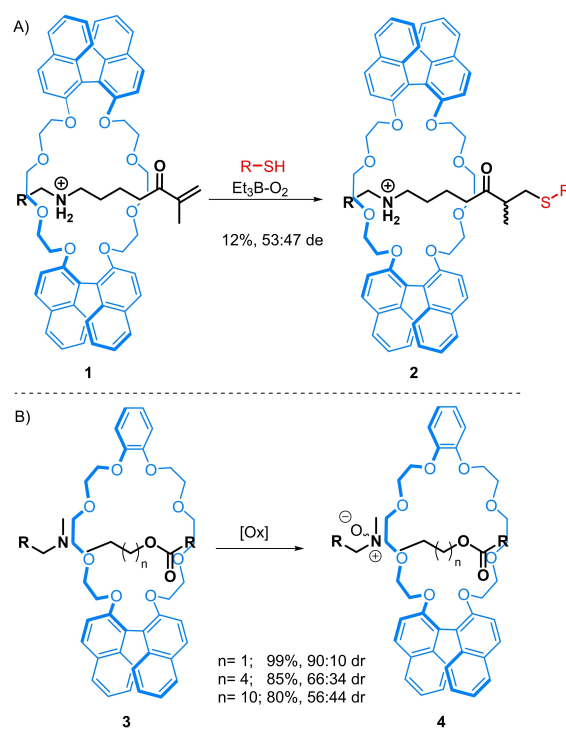
are oriented (excluding *meso* forms). Instead, the presence of axial or planar stereogenic elements do not necessarily result in an oriented ring. As a result, rotaxanes formed by combination of this type of macrocycles with  $C_{nv}$  threads will contain elements of both covalent and mechanical stereochemistry.<sup>[3]</sup> The most illustrative examples of this type of species are rotaxanes containing cyclodextrins (with at least 30 stereogenic centers) as a rigid ring component.<sup>[14]</sup> Although such MIMs are probably contemplated as orientational isomers, due to the cone shape of its ring component, they are better qualified as mechanically planar chiral diastereoisomers. Thus, cyclodextrins have been extensively employed for the selective assembly of chiral oriented rotaxanes<sup>[15–21]</sup> or as nanoreactors for performing asymmetric processes in their cavity.<sup>[22–26]</sup> Having these precedents in mind, we envisaged that polyamide macrocycles, quite habitual ring components of [2]rotaxanes, incorporating a chiral carbon atom, could also be used to develop synthetically useful chirotopic environments (Figure 1C).

Whereas [2]rotaxanes containing chiral elements at the thread are more or less habitual in the literature,<sup>[3,5]</sup> those containing stereogenic elements at the ring have been scarcely reported. In most of these latter species, the stereogenic unit at the ring is an enantioenriched binaphthyl unit<sup>[27]</sup> which imposes a chiral environment useful for inducing a chiroptical response to an achiral thread,<sup>[28]</sup> for controlling the helical twisting of a polyacetylene macromolecule<sup>[29]</sup> and for achieving enantioselective transformations when used as catalysts.<sup>[30,31]</sup>

When the axial chirality of these rings is combined with chiral threads, the multipoint interactions between the mechanically linked components are in the origin of the good anion binding enantioselectivities achieved by such species,<sup>[32]</sup> and it has been also shown to determine useful kinetic effects of its diastereoisomerism on dethreading rates.<sup>[33]</sup> More relevant for our present work, being probably the only related precedents, are two reports by Takata in which a chiral binaphthyl unit at the ring of a rotaxane **1** or **3** influences the outcome of two different reactions occurring at the thread to give **2** and **4** in a moderate to good diastereoselective manner (Scheme 1).<sup>[34,35]</sup>

In contrast, the introduction of point chirality at the macrocyclic component of [2]rotaxanes is very rare. Leigh have disclosed such a case bearing two consecutive chiral carbon atoms (belonging to a *trans*-1,2-cyclohexanediamine fragment) at the ring of a [2]rotaxane, that was used for improving the catalytic performance shown by the isolated ring component in an enantioselective transformation.<sup>[36]</sup> Another example described as a racemic mixture is the synthesis of directional isomers of crown ether-based [2]rotaxanes described by Takata and collaborators.<sup>[37]</sup>

We have recently described the chemical consequences of the mechanical bond on the base-promoted intramolecular cyclization of interlocked fumaramides **5** (Scheme 2A).<sup>[38–40]</sup> Starting from kinetically stabilized *N*-benzylfumaramide-based [2]pseudorotaxanes, we efficiently accessed the non-interlocked  $\beta$ -lactams **6** in a regio- and diastereoselective fashion, after a cyclization and dethreading reaction. Moreover, the presence of a chiral  $\alpha$ -methyl



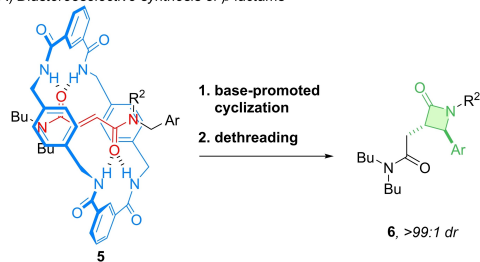
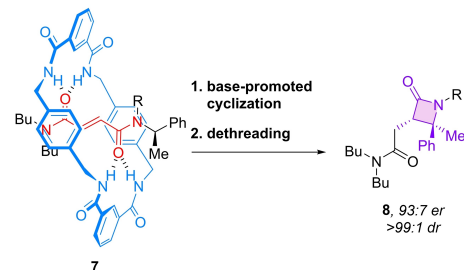
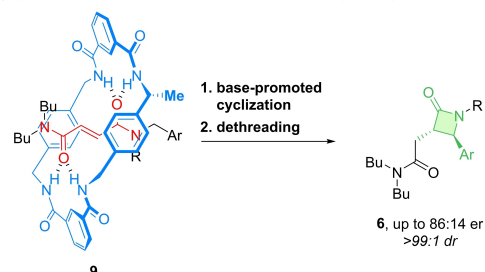
**Scheme 1.** Diastereoselective functionalization of a [2]rotaxane where the chiral macrocycle induces: A) a marginally diastereoselective end-capping reaction of the thread in pseudorotaxane **1**;<sup>[34]</sup> B) a selective oxidation to afford a diastereomeric mixture of rotaxanes **4**.<sup>[35]</sup>

R = 3,5-*t*Bu<sub>2</sub>C<sub>6</sub>H<sub>3</sub>

benzyl group on the fumaramide thread allowed the isolation of optically active  $\beta$ -lactams **8** (Scheme 2B). In this transformation, the chiral information present at the thread in rotaxanes **7** is maintained during the formation of the new quaternary stereogenic center in the lactam **8**, occurring with retention of the initial configuration.<sup>[41]</sup>

We herein describe a novel traceless strategy to yield enantioenriched  $\beta$ -lactams by using the *N*-(arylmethyl)fumaramide-based [2]pseudorotaxanes **9**, having a macrocycle with a stereocenter with a defined chirality (Scheme 2C). When the chiral polyamide macrocycle having a stereogenic center surrounds a non-symmetrical fumaramide, a pair of enantioenriched orientational mechanostereoisomers (two diastereoisomers with mechanically planar and covalent chirality, Figure 1C) can be obtained. These systems were evaluated as substrates in the base-induced intramolecular cyclization of the thread, with the aim of obtaining *trans*- $\beta$ -lactams **6** in an enantiomeric fashion. Thus, the chiral information could be transferred through the space, from the ring to the axis, during the 4-exo-cyclization to control the formation of the two contiguous stereogenic centers at the final  $\beta$ -lactam cores. Moreover, other enantioenriched valuable compounds, such as  $\beta$ -amino acids and  $\gamma$ -lactams, could also be accessed by following this methodology.

The reactions shown in Scheme 1 are probably the only two examples known of diastereoselective post-synthetic modification of the achiral thread carried out under the

A) Diastereoselective synthesis of  $\beta$ -lactamsB) Enantioselective synthesis of  $\beta$ -lactams through covalent chirality inductionC) Synthesis of enantioenriched *trans*- $\beta$ -lactams through a ring-to-thread chirality transfer process

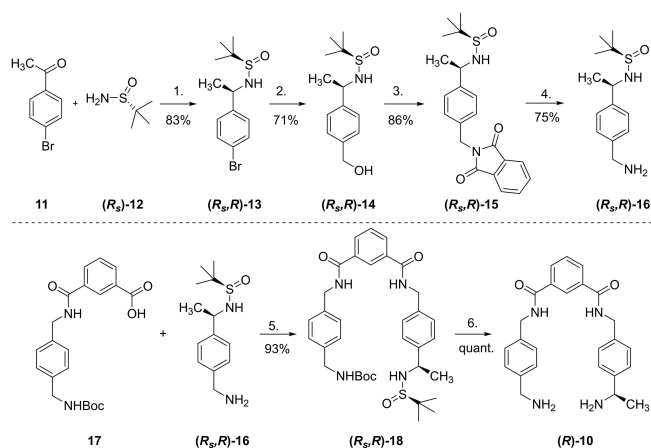
**Scheme 2.** Base-promoted cyclization of: A) *N*-benzylfumaramide-based [2]pseudorotaxanes **5** in a diastereoselective manner;<sup>[38]</sup> B) enantiopure *N*- $\alpha$ -(methylbenzyl)fumaramide-based [2]pseudorotaxanes **7**;<sup>[41]</sup> C) an orientational mechanostereoisomer **9** in an enantioselective fashion (*this work*).

chiral influence of the ring, with axially chiral binaphthyl units, in a [2]rotaxane<sup>[42,43]</sup> In this manuscript we disclose our results on approaching a similar strategy by using another type of stereogenic inductor, point chirality (*only a single chiral carbon atom!*), placed at the macrocycle of a [2]rotaxane, and a different diastereoselective transformation occurring at the thread.

## Results and Discussion

### Synthesis of the kinetically stable pseudo[2]rotaxanes **9**

To obtain the enantiopure kinetically stable pseudo-[2]rotaxanes **9**, we synthesized the enantioenriched “U”-shaped intermediate **10**, bearing a chiral benzylic stereocenter (*R* absolute configuration) (Scheme 3). The synthetic route for (*R*)-**10** started with a one-pot condensation-reduction protocol<sup>[44]</sup> between 4-bromoacetophenone **11** and the enantiopure (*R<sub>S</sub>*)-2-methyl-2-propanesulfinamide **12**, affording the (*R<sub>S</sub>*)-sulfinamide **13** as a single diaster-

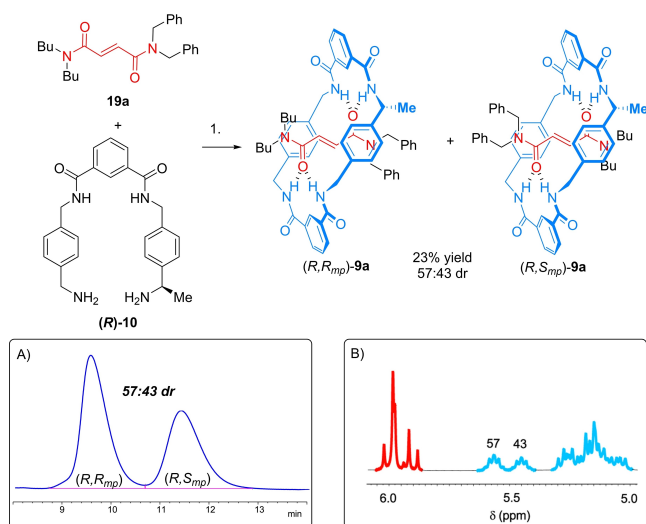


**Scheme 3.** Synthesis of the enantiopure “U”-shaped precursor (*R*)-**10**. Reagents and conditions: 1) (i) Ti(OEt)<sub>4</sub>, 75 °C, 15 h; (ii) NaBH<sub>4</sub>, –50 °C to 25 °C, 15 h; 2) (i) *n*-BuLi, THF, –78 °C, 10 min, then DMF, 25 °C, 1 h; (ii) NaBH<sub>4</sub>, 2 h, 25 °C; 3) phthalimide, PPh<sub>3</sub>, diethyl azodicarboxylate, THF, 25 °C, 24 h; 4) hydrazine hydrate, THF:EtOH (9:1), reflux, 18 h; 5) EDCI, DMAP, CH<sub>2</sub>Cl<sub>2</sub>, 25 °C, 48 h; 6) (i) HCl 6 M in dioxane, MeOH, 25 °C, 3 h; (ii) Amberlyst A21<sup>®</sup>, CH<sub>2</sub>Cl<sub>2</sub>:MeOH (4:1), 25 °C, 3 h.

oisomer in high yield. A bromo-lithium exchange, followed by the addition of dimethylformamide and the ulterior reduction with NaBH<sub>4</sub>, afforded alcohol **14** in 71 % yield. The Mitsunobu reaction of alcohol **14** with phthalimide yielded compound **15**, which was converted into the primary amine **16** by reaction with hydrazine. The coupling of the amine **16** with the carboxylic acid **17** (see Supporting Information for full synthetic details) yielded the protected “U”-shaped compound **18**, which was transformed in the diamine (*R*)-**10** quantitatively.

Diamine (*R*)-**10** was straightforwardly employed in the three-component clipping reaction<sup>[45]</sup> in the presence of the non-symmetric fumaramide-based thread **19a** and isophthaloyl dichloride (Scheme 4). A mixture of the two possible mechanically interlocked epimers (*R,R<sub>mp</sub>* and *R,S<sub>mp</sub>*) of **9a** was obtained with a diastereomeric ratio of 57:43 dr, determined by both analytical HPLC and <sup>1</sup>H NMR (Scheme 3, insets A and B), revealing a small induction in favour of the (*R,R<sub>mp</sub>*) isomer (*vide infra*). The presence of the small methyl group on the diamine (*R*)-**10** shows almost ineffective in controlling the recognition process with the thread **19a** before the clipping reaction occurs, as expected in advance, due to the high flexibility of the diamine intermediate.

The separation of both diastereoisomers of **9a** was next attempted, initially by a dethreading reaction of the mixture of rotaxanes **9a**. If the two diastereoisomers would have different rates towards the separation of the interlocked components, the isolation of one of them could be feasible.<sup>[33]</sup> Thus, we monitored the deslipping reaction of rotaxanes **9a** in DMF-*d*<sub>7</sub> at 25 °C by <sup>1</sup>H NMR (Figure S2), finding that the minor diastereoisomer was slightly more stable than its mechanical epimer. Disappointingly, the difference of the stability was not large enough to obtain the more stable isomer as a single compound. Nevertheless, we



**Scheme 4.** Synthesis of the mechanically planar chiral rotaxanes **9a** as a mixture of diastereoisomers (57:43 dr). Reagents and conditions: 1) isophthaloyl dichloride, Et<sub>3</sub>N, CHCl<sub>3</sub>, 25 °C, 4 h. Diastereomeric ratio determined by <sup>1</sup>H NMR spectroscopy and HPLC. Insets: A) HPLC chromatogram of the mixture of rotaxanes **9a** (Chiralpak IC-3 column, 95:5 CH<sub>2</sub>Cl<sub>2</sub>:iPrOH, 0.5 mL min<sup>-1</sup>, 254 nm); B) Partial <sup>1</sup>H NMR spectra of the mixture of rotaxanes **9a** (400 MHz, CDCl<sub>3</sub>, 273 K). Signals related to the fumaramide double bond are highlighted in red. Signals related to the macrocycle are highlighted in light blue.

were able to hardly separate both diastereoisomers by preparative TLC after several iterations (see Supporting Information for further details).<sup>[46]</sup> The structure of the minor diastereoisomer was elucidated by X-ray single-crystal diffraction (Tables S4–S5).<sup>[47]</sup> We found that the methyl group at the macrocycle (*R* configuration) in this isomer is placed nearby the butyl groups of the thread (Figure 2 and Figure S3). This orientation allowed the establishment, on the solid state, of  $\pi$ – $\pi$  aromatic interactions between one isophthalamide unit and one of the terminal benzyl groups, together with CH– $\pi$  interactions between the second

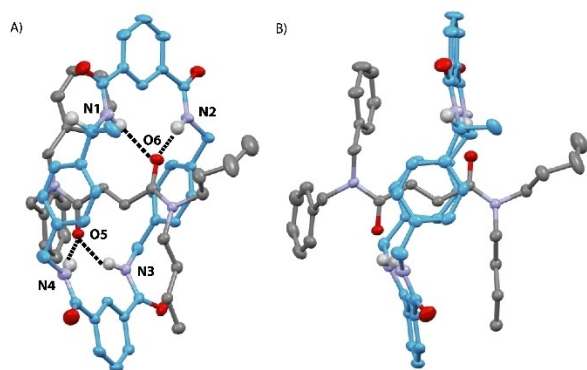
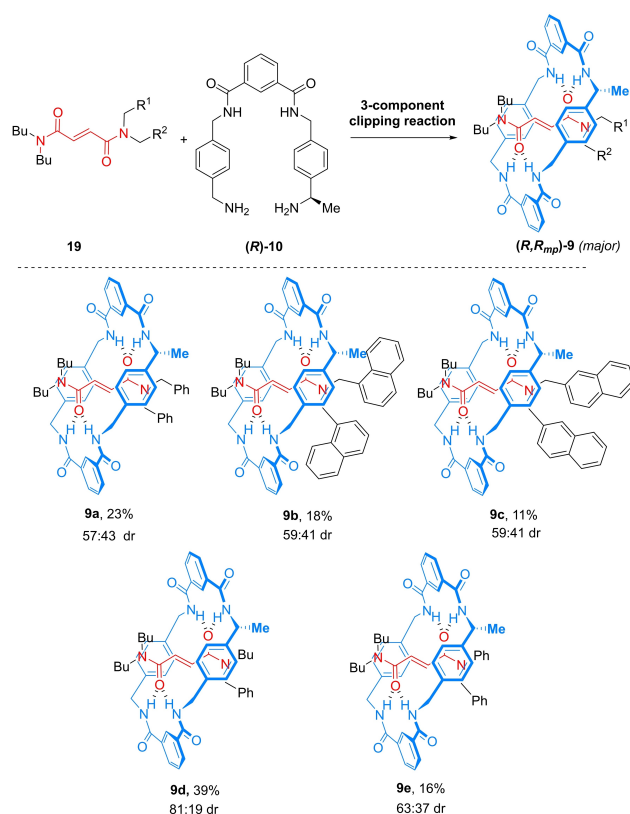


**Figure 2.** X-ray structure of rotaxane (*R,S<sub>mp</sub>*)-**9a** (minor diastereoisomer).<sup>[47]</sup> A) inclined view; B) side view. Intramolecular hydrogen-bond lengths [Å] (and angles [°]): N1–H01–O6 2.41 (171.3); N2–H02–O6 2.16 (167.9); N3–H03–O5 2.24 (159.5); N4–H04–O5 2.21 (164.8).

isophthalamide group and one butyl group.<sup>[48]</sup> In the crystal, the methyl group at the ring adopts the most energetically favoured pseudo axial position.<sup>[49]</sup> Following the CIP rules,<sup>[3]</sup> we assigned the relative configuration of this compound as (*R,S<sub>mp</sub>*)-**9a** (minor diastereoisomer).

Aimed to explore the effect of the incorporation of the stereogenic center at the ring on the stereochemical course of the cited 4-exo intramolecular cyclization at the thread, we synthesized a series of fumaramide-based rotaxanes **9** by changing the nature and bulkiness of the stoppers placed at the end of threads **19** (Scheme 5). By using the enantiopure “U”-shaped diamine (*R*)-**10**, we obtained some other rotaxanes **9** as mixtures of diastereoisomers, in all cases in moderate yields. Interestingly the stereoselectivity reached in the case of rotaxane **9d** was remarkable (81:19 dr). The choice of the ArCH<sub>2</sub> groups (Ar = phenyl, 1-naphthyl or 2-naphthyl) at the threads is intended to allow the base-promoted intramolecular cyclization of the respective threads. The placing of two butyl groups at one of the stoppers of the fumaramide thread would enable the easy removal of the putative resulting lactam from the macrocyclic component under thermal conditions.<sup>[50,51]</sup>

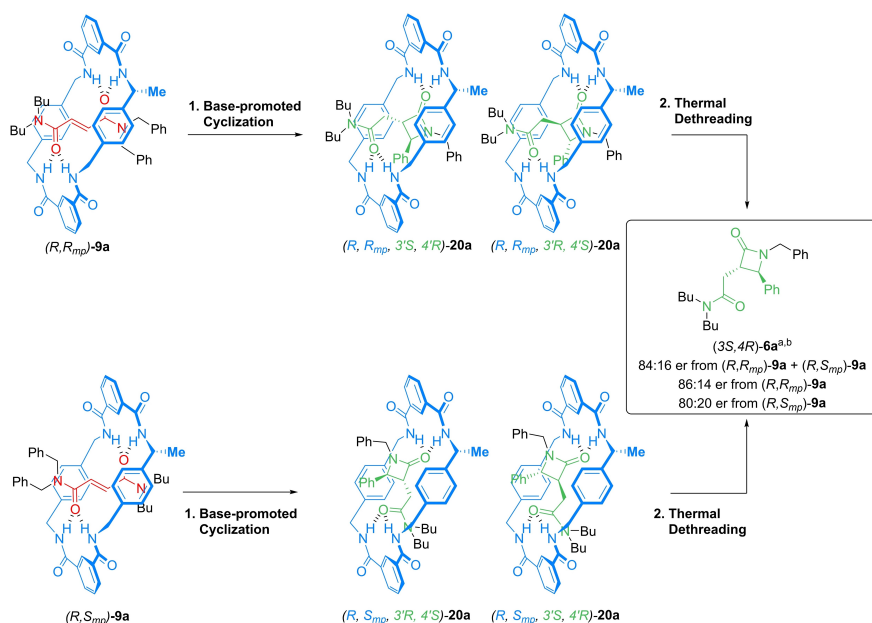


**Scheme 5.** Synthesis of the mechanically planar chiral rotaxanes **9** as mixtures of diastereoisomers through a 3-component clipping reaction. Reagents and conditions: isophthaloyl chloride, Et<sub>3</sub>N, CHCl<sub>3</sub>, 25 °C, 4 h. Diastereomeric ratio determined by HPLC.



Base-Promoted Cyclization of the [2]Rotaxanes **9**

The base-promoted intramolecular cyclization of the chiral fumaramide-based rotaxane **9a** (57:43 dr) could generate eight diastereoisomers of the interlocked  $\beta$ -lactam **20a**. The four *trans*-**20a** are shown in Scheme 6. The first attempt of the cyclization process for **9a** was accomplished starting from the mixture of diastereoisomers (57:43 dr) in the presence of CsOH and DMF as solvent at 25 °C, observing the formation of a very complex mixture of compounds (by TLC), attributed to the presence of several diastereoisomeric interlocked lactams **20a**, which could not be isolated separately. Attempts to determine the ratio of these diastereoisomers by <sup>1</sup>H NMR resulted unfruitful. Aimed to simplify the data and analyse the process outcome, we performed a dethreading reaction of the mixture of interlocked lactams **20a**, smoothly affording the *trans*- $\beta$ -lactam **6a** as a unique diastereoisomer (the *cis* isomer of **6a** was not detected). To our delight, **6a** was enantiomerically enriched, with a 78:22 enantiomeric ratio (er) shown by chiral HPLC. After optimizing the reaction conditions with the epimeric mixture of **6a** (solvent, base and temperature, see Supporting Information for further details, Tables S1–S3), we selected DMF and CsOH as the optimal combination of solvent and base. The excess of base employed in the experiments and the low temperature preserved the mechanical bond in the kinetically stabilized pseudorotaxane **9a**, precluding the dethreading process (the presence of the free thread was not observed in the screening experiments).<sup>[38,40]</sup> Moreover, decreasing the reaction temperature to 0 °C gave an improved 84:16 er of the *trans*- $\beta$ -lactam **6a**. With the optimized reaction conditions settled,



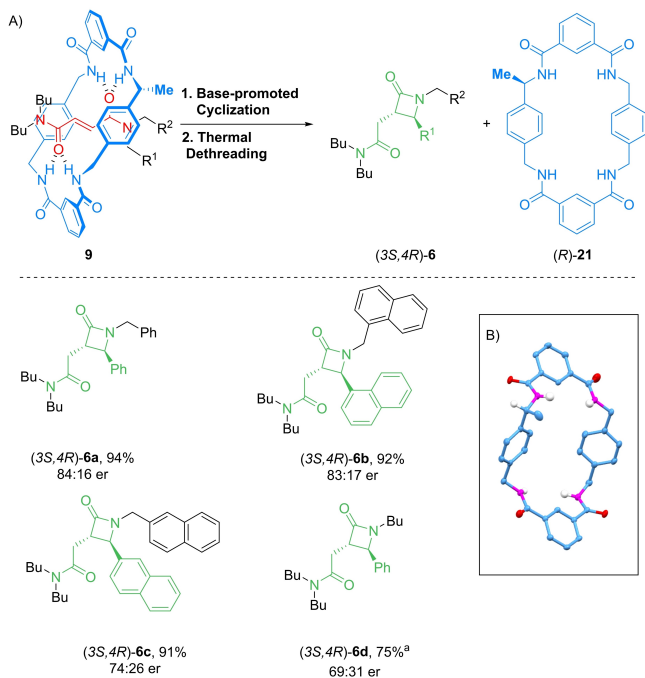
**Scheme 6.** CsOH-promoted cyclization of rotaxanes **9a** followed by a thermal dethreading. The base-promoted cyclization of both mechanical epimers **9a** can yield the four possible diastereoisomers of the interlocked *trans*- $\beta$ -lactams **20a**. After dethreading, the enantioenriched *trans*- $\beta$ -lactam **6a** is obtained. Reagents and conditions: 1) CsOH (8 equiv), DMF, 0 °C, 4 days; 2) DMF, 80 °C, 12 h. <sup>a</sup> Absolute configuration determined by derivatization of **6a** (see Supporting Information). <sup>b</sup> Enantiomeric ratio determined by chiral HPLC.

we next performed the cyclization for each separated diastereoisomer of **9a**. Starting from (*R,R<sub>mp</sub>*)-**9a** (major diastereoisomer, initial 97:3 dr), the lactam **6a** was obtained in an 86:14 er. The cyclization of the minor diastereoisomer (*R,S<sub>mp</sub>*)-**9a** (initial 5:95 dr) also led mainly to the same enantiomer of **6a**, although with a slightly lower er (80:20). Thus, the cyclization of both diastereoisomers of **9a**, differing only on its orientational mechanoisomerism, majorly yielded the same enantiomer of lactam **6a** with nearby level of enantiocontrol. In both diastereoisomers, the base-induced cyclization seems to occur through a nucleophilic attack of the benzylic anion to the *Re,Re* face of the double bond, apparently the less hindered one. At this point it is important to highlight that these type of kinetically stabilized pseudorotaxanes with butyl groups at the ends, as **9**, do not experience any dethreading-threading process in competitive hydrogen-bonded solvents such as DMF. This scenario is crucial to exclude any possibility in which the free thread could slip inside the macrocycle by the other side, in an epimerization process switching the chiral environment.<sup>[52]</sup>

In addition, the cyclization of non-interlocked fumaramide **19a** in the presence of free macrocycle (*R*)-**21** (1 equiv) under the same reaction conditions was carried out, finding the formation of the *trans*-lactam **6a**, together with the expected *cis*-**6a**, as a racemate (Figure S5). The slippage of two polarophobic alkyl chains (butyl groups) inside the polar cavity of the ring is highly disfavoured, as it has been found in previous studies. Thus the non-interlocked macrocycle cannot control the enantioselectivity of the process when occurs out of its cavity.<sup>[38,53]</sup>

These results demonstrate that: (i) the incorporation of just one stereocenter at one out of four methylenic positions of the macrocycle is enough to efficiently control the stereochemical course of the cyclization of the *N*-benzylfumaramide through the confined space of the mechanical bond of a benzylic amide [2]rotaxane; and (ii) the observed chiral induction seems to be controlled mainly by the covalent stereogenic center, which is kept fixed in all the experiments, rather than by the mechanical planar stereogenic unit. Thus, the subtle decrease of the symmetry of the [2]rotaxane due to the incorporation of the methyl group at only one of the benzylic carbons of the ring is shown to have a rather neglecting influence on the overall mechanically planar discrimination of the systems, but is however enough to promote a notably controlled chirality transfer from the ring to the thread.

Having in mind that both enantioenriched diastereoisomers of rotaxane **9a** yielded the same enantiomer of lactam **6a** upon cyclization-dethreading, and that the physical separation of each orientational epimer is highly challenging, we decided to proceed with the cyclization reaction of the other rotaxanes **9b–d** as diastereomeric mixtures (Scheme 7A). For simplicity, we carried out a one-pot protocol, including the initial CsOH-promoted cyclization of the systems at low temperature, followed by a neutralization step with 1 M HCl, and ulterior heating at 80 °C to release the lactam from the interlocked structure. Following this methodology, we smoothly isolated the enantioenriched *trans*- $\beta$ -lactams **6a–c** (er between 84:16 and 74:26) in good to excellent yields. The formation of the

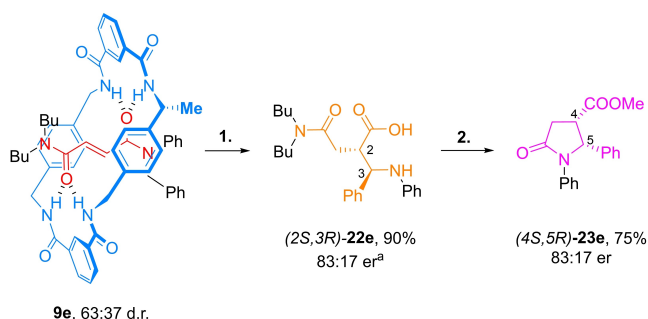


**Scheme 7.** One-pot synthesis of the enantioenriched *trans*- $\beta$ -lactams **6**. A) Substrate scope; B) X-ray structure of macrocycle (*R*)-**21**.<sup>[47]</sup> Reagents and conditions: 1) CsOH (8 equiv), DMF, 0 °C, 4 days; 2) (i) HCl (1 M), pH = 7; (ii) 100 °C, 8 h. Enantiomeric ratio determined by chiral HPLC. <sup>a</sup> Reaction performed at 25 °C for 2 days.

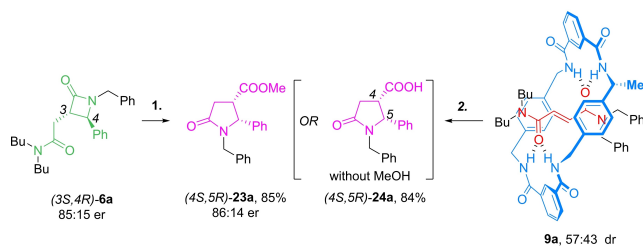
corresponding *cis* isomer was not observed in any case, thus highlighting the important role of the mechanical bond for controlling the selectivity of this process. The tributylfumaramide-based rotaxane **9d** proved to be unreactive at low temperature. Therefore, we performed the reaction at 25 °C, isolating the lactam **6d** in a moderate yield with lower enantioselectivity (69:31 er). In addition, the chiral macrocycle (*R*)-**21** was also isolated in all the cases at the end of the cyclization-dethreading protocol. We were able to elucidate its structure at the solid state by single-crystal XRD<sup>[47]</sup> (Scheme 7B and Figure S4), proving that it did not racemize during the cyclization-dethreading protocol. Note that the methyl group adopts a pseudoaxial disposition (Tables S6–S7) similar to that found in the crystal structure of rotaxane (*R,S<sub>mp</sub>*)-**9a**.

The case of rotaxane **9e** was peculiar. *N*-Phenyl-substituted  $\beta$ -lactams are known to suffer a ring-opening reaction in basic media, affording the corresponding  $\beta$ -amino acids.<sup>[54]</sup> In our previous report on the synthesis of  $\beta$ -lactams from interlocked fumaramides, we isolated an interlocked  $\beta$ -amino acid from the cyclization reaction of a mechanized *N,N*-benzylphenylfumaramide.<sup>[38]</sup> Thus, we employed rotaxane **9e** (as mixture 63:37 of diastereoisomers) as starting material, which triggers the formation of the non-interlocked enantioenriched  $\beta$ -amino acid **22e** (*anti* diastereoisomer) in high yield following the one-pot protocol described before (Scheme 8). In order to measure the enantiomeric excess of amino acid **22e**, we decided to prepare its corresponding methyl ester. Remarkably, the reaction of the  $\beta$ -amino acid **22e** in MeOH and in the presence of acid yielded the methylated *cis*- $\gamma$ -lactam **23e**,<sup>[55]</sup> instead of the expected methyl amino ester, observing the release of dibutylamine in the <sup>1</sup>H NMR spectra of the reaction crude. We assumed that the enantiomeric ratio of **23e** (83:17 er) was the same as the parent **22e** (not measured).

Furthermore, we also prepared the *cis*- $\gamma$ -lactam **23a**<sup>[56]</sup> as a single diastereoisomer starting from the non-interlocked  $\beta$ -lactam **6a** under the same conditions (Scheme 9), importantly maintaining the enantiomeric excess of the initial azetidinone **6a** (86:14 er). The reaction of azetidinone **6a** in the absence of methanol (DMSO as the sole solvent) yielded



**Scheme 8.** Synthesis of the enantioenriched  $\beta$ -amino acid **22e** and the  $\gamma$ -lactam **23e**. Reagents and conditions: 1) (i) CsOH (8 equiv), DMF, 0 °C, 4 days, then extraction with AcOEt; 2) HCl (1 M), MeOH, 65 °C, 24 h. Enantiomeric ratio taken from the methylated  $\gamma$ -lactam **23e**.



**Scheme 9.** Synthesis of the enantioenriched *cis*- $\gamma$ -lactams **23 a** and **24 a**. Reagents and conditions: 1) HCl 1 M, DMSO:MeOH (1 : 1), 100 °C, 24 h; 2) (i) CsOH, DMF, 0 °C, 4 days; (ii) HCl (1 M), pH = 1, DMF:MeOH (1 : 1), 100 °C, 24 h. Enantiomeric ratio determined by chiral HPLC.

the lactam **24 a** with a free carboxylic acid (Scheme S3, for a proposed mechanism of this transformation see Scheme S5). Importantly, the *cis*- $\gamma$ -lactams **23 a** or **24 a** can also be obtained directly from the rotaxanes **9 a**, by following a one-pot procedure: base-promoted cyclization, acidification until pH < 1 and further heating, not observing an important decrease on the yield or enantiomeric excess (see Scheme S4).  $\gamma$ -Lactam **24 a** was used for the determination of the absolute configuration of the synthesized compounds, assuming a uniform reaction mechanism in all the cases. The esterification of **24 a** with a chiral phthalimide and the posterior NMR analyses of the obtained diastereoisomers<sup>[57]</sup> allowed us to conclude that the absolute configuration of the main enantiomer of the  $\gamma$ -lactam **24 a** was (4*S*, 5*R*). Thus, the main isomer of the starting  $\beta$ -lactam is (3*S*,4*R*)-**6 a** (Figure S1 and Scheme S6).

### Computational Studies of the Cyclization Process

In search of an explanation on how the transfer of the chiral information from the ring to the thread occurs, computational studies on this cyclization process were carried out (see Supporting Information for further details). Thus, we analysed the key cyclization process for leading to the enantioenriched *trans*-lactams (3*S*,4*R*)-**6** by computational methods at the (SMD, DMF)RI-SCS-MP2/ma-def2-svp//wB97XD/def2-SVP theoretical level. The pathway previously computed for the cyclization of *N*-benzylfumaramide-based [2]rotaxanes towards interlocked lactams was assumed.<sup>[40]</sup> We predicted there that the selective formation of the *trans*-lactams **6** rather than the *cis*-lactams **6**, not observed experimentally, was due to the larger number of non-covalent interactions established between the two components, macrocycle and thread, together with the minor structural deformation of the macrocycle adopted in the *trans*-cyclization step when compared with the *cis*-cyclization. With this premise in our hands, we computed the two possible *trans*-cyclization steps of two simplified chiral mechanically interlocked *N,N*-dibenzyl-*N,N'*-dimethylfumaramides finding that, in both cases, the lowest energy cyclization is that conducting ((3*S*,4*R*)-**TS**<sub>*R,Rmp*</sub> and (3*S*,4*R*)-**TS**<sub>*R,Smp*</sub>) to the interlocked *trans*-lactams (3*S*,4*R*)-**INT2**, that evolve to the *trans*-lactams (3*S*,4*R*)-**25** (Figure 3A, for full

details see Supporting Information, Scheme S7 and Figures S6–S7). However, the rationalization of the favourable computed cyclization mode turns more intricate due to the similar geometrical parameters, such as bond lengths and angles, between the complementary transition structures and the presence of multiple non-covalent interactions between macrocycle and thread (Figures S8–S9). Thus, we analysed in detail the energy difference,  $\Delta\Delta E^\ddagger$ , between both transition states with the same mechanically planar chirality, (3*S*,4*R*)-**TS**<sub>*R,Rmp*</sub> vs. (3*R*,4*S*)-**TS**<sub>*R,Rmp*</sub> and (3*S*,4*R*)-**TS**<sub>*R,Smp*</sub> vs. (3*R*,4*S*)-**TS**<sub>*R,Smp*</sub>, by splitting them in their main contributions provided by the difference in the energy of the threads,  $\Delta\Delta E_{\text{thread}^\ddagger}$  and of the macrocycles,  $\Delta\Delta E_{\text{mac}^\ddagger}$  and also in the interaction energies between both of them,  $\Delta\Delta E_{\text{int}^\ddagger}$  [in their respective **TS** geometries, see Eq. (1)]. A similar energy decomposition approach has been widely used to explain the enantioselective ratios of the products in related asymmetric catalysed processes.<sup>[58–60]</sup>

$$\Delta\Delta E^\ddagger = \Delta\Delta E_{\text{int}^\ddagger} + \Delta\Delta E_{\text{thread}^\ddagger} + \Delta\Delta E_{\text{mac}^\ddagger} \quad (1)$$

Regarding both **TS**<sub>*R,Rmp*</sub> transition states, the transition structure (3*S*,4*R*)-**TS**<sub>*R,Rmp*</sub>, which leads to the major enantiomer of the *trans*-lactams **6**, is 6.6 kJ mol<sup>−1</sup> more stable than (3*R*,4*S*)-**TS**<sub>*R,Rmp*</sub>. Whereas no significant differences are observed in the energies of the macrocycle and in those of the interaction energies, the geometry adopted by the thread inside of the chiral cavity at the (3*S*,4*R*)-**TS**<sub>*R,Rmp*</sub> is stabilized by 7.8 kJ mol<sup>−1</sup> respect to that at the (3*R*,4*S*)-**TS**<sub>*R,Rmp*</sub> (Figure 3B). In this sense, the methyl group, which points towards the reactive cyclization site of the thread, might somehow disturb the cyclization in the unfavourable transition structure (3*R*,4*S*)-**TS**<sub>*R,Rmp*</sub>. In contrast, the energy differences between the components of both structures corresponding to **TS**<sub>*R,Smp*</sub> structures are minimal,  $\Delta\Delta E^\ddagger = 0.9$  kJ mol<sup>−1</sup> in favour of the (3*S*,4*R*)-**TS**<sub>*R,Smp*</sub>, being the principal contribution originating from the difference in their interaction energies  $\Delta\Delta E_{\text{int}^\ddagger} = +2.0$  kJ mol<sup>−1</sup> (Figure 3C). Note that in these later transition states the pendant methyl group is pointing away from the place in which the four-membered ring is forming, and therefore its steric influence on the cyclization fashion might be minimal. The minor difference between the couple of transition structures **TS**<sub>*R,Smp*</sub> with respect to its mechanical epimers **TS**<sub>*R,Rmp*</sub> might be responsible for the lower enantiomeric excess observed in the *trans*-lactam **6 a** when the minor diastereoisomer of [2]rotaxane (*R,Smp*)-**9 a** was used as starting material.

The interaction energy is the result of the qualitative contribution of diverse and individual non-covalent interactions between the thread and the macrocycle. Thus, we divided the macrocycle into four representative motifs, two isophthalamide fragments and two aromatic sidewalls and scrutinized their interactions with the entire thread (Table S8–S9 and Figures S10–S13). We computed that the interaction energies due to the establishment of hydrogen bonds between the isophthalamide fragments and the carbonyl groups of the thread are similar in both complementary transition structures. Whereas there are non-significant differences in the computed interaction energies

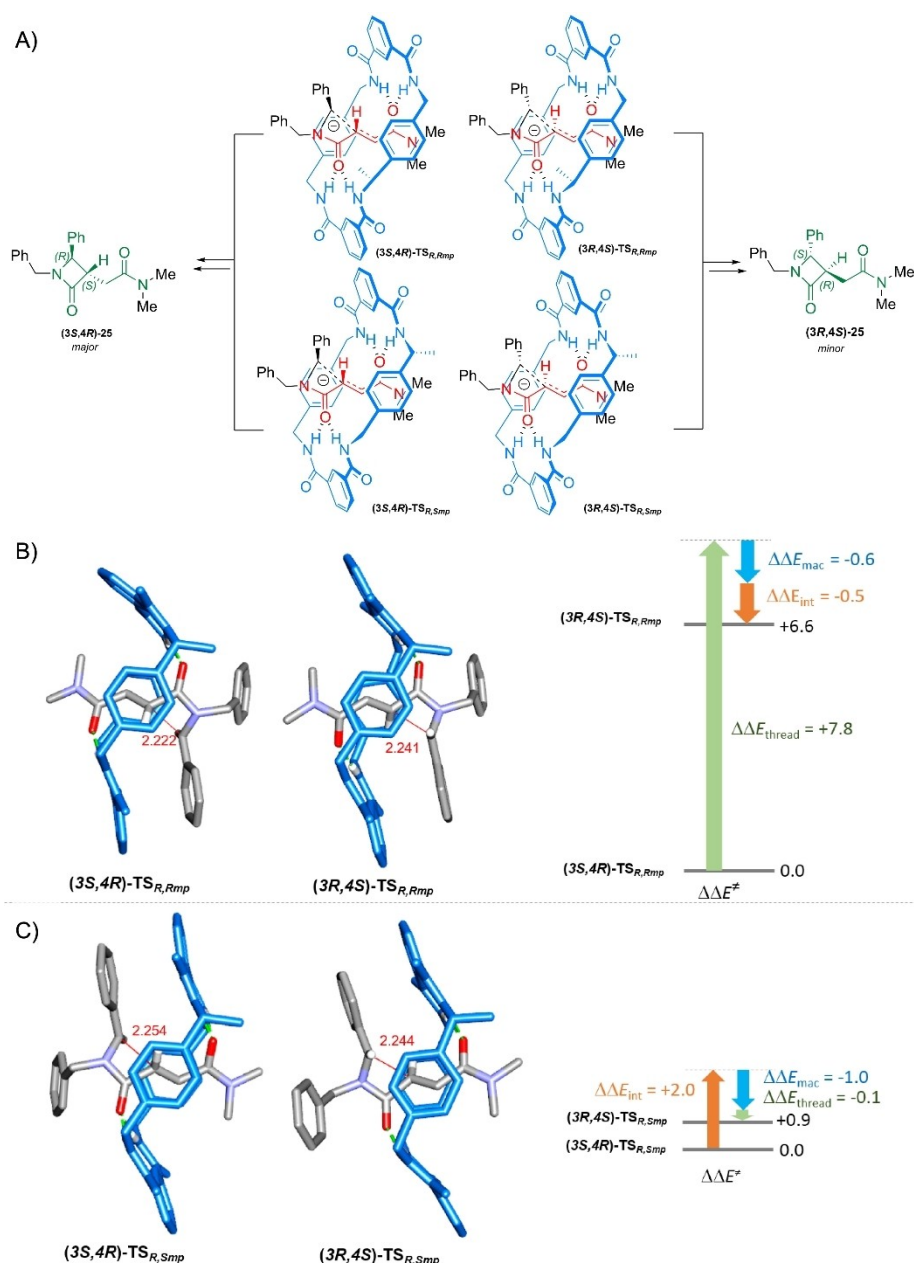


**Figure 3.** Computed transition structures of: A) Chemical diagrams of the four possible transition states **TS** (same orientation of the thread) for the cyclization step; B)  $(3S,4R)\text{-TS}_{R,Rmp}$  and  $(3R,4S)\text{-TS}_{R,Rmp}$  for the cyclization step (same orientation of the macrocycle) and decomposition of the energy difference between  $(3R,4S)\text{-TS}_{R,Rmp}$  and  $(3S,4R)\text{-TS}_{R,Rmp}$  ( $\Delta\Delta E^\ddagger$ ) into contributions from the energy difference of the macrocycles ( $\Delta\Delta E_{mac}$ ) and threads ( $\Delta\Delta E_{thread}$ ) and also between the interaction energies of the thread with the macrocycle ( $\Delta\Delta E_{int}$ ); C)  $(3S,4R)\text{-TS}_{R,Smp}$  and  $(3R,4S)\text{-TS}_{R,Smp}$  (same orientation of the macrocycle) and analogous decomposition of the difference in energies between  $(3R,4S)\text{-TS}_{R,Smp}$  and  $(3S,4R)\text{-TS}_{R,Smp}$ . Energies are shown in  $\text{kJ mol}^{-1}$  and distances in angstroms.

between the non-substituted sidewall and the thread, large differences were observed in the dispersive and  $\text{CH}\cdots\pi$  interactions between the thread and the methyl-substituted aromatic sidewalls of the macrocycle. The analysis of this particular interaction revealed that the aromatic sidewall interacts larger with the thread at the  $(3R,4S)\text{-TS}$  geometry than at the  $(3S,4R)\text{-TS}$  disposition. As expected, this fact reveals that the presence of the methyl group at the

macrocycle plays the important role in the enantioselective course of the reaction.

This analysis should be taken as a qualitative approach<sup>[11]</sup> to the experimental model as other non-covalent interactions could be involved, such as the  $\text{CH}\cdots\pi$  interaction between the butyl chains with the nearby isophthalamide ring,<sup>[47]</sup> not evaluated herein. So, the sum of several factors, such as the geometry adopted by the thread inside the chiral cavity together with the subtle difference interactions



between the thread and the macrocycle in the complementary transition structures (3*S*,4*R*)-**TS** and (3*R*,4*S*)-**TS**, are behind the favoured cyclization mode of the interlocked *N,N*-benzyl-substituted fumaramides.

## Conclusion

We have incorporated, for the first time, point chiral information to a polyamide macrocycle present in kinetically-stabilized hydrogen-bonded pseudorotaxanes. When this macrocycle surrounds a non-symmetrical thread, two oriented mechanoisomers are obtained, differing on the orientation of the thread. These systems enabled the study of the chirality transfer through the mechanical bond on the diastereoselective intramolecular cyclization of the interlocked fumaramides towards enantioenriched  $\beta$ -lactams. This traceless chiral auxiliary approach allows to obtain enantioenriched  $\beta$ -lactams, inaccessible by cyclization of chiral interlocked fumaramides bearing the chiral information at the axis.<sup>[41]</sup> The base-promoted cyclization of each interlocked mechanical epimer, followed by a dethreading protocol, yielded the same enantiomer of the *trans*- $\beta$ -lactam. This result points out that the enantioselectivity of the process is controlled only by the covalent stereogenic center, fixed in all our experiments, rather than also by the mechanical planar stereogenic unit. This protocol was expanded to the cyclization of a series of interlocked fumaramides with different substitutions. Moreover, an enantioenriched  $\beta$ -amino acid was also obtained by using an interlocked *N*-phenylsubstituted derivative. The acid-catalysed intramolecular transamidation reaction of the  $\beta$ -lactam and amino acid derivatives produced the corresponding enantioenriched *cis*- $\gamma$ -lactams, without racemization. The absolute configuration of the prepared 2-azetidinones was elucidated both experimentally and rationalized with the aid of computational studies. Our calculations predicted that the transition structures leading to the lactams (3*S*,4*R*)-**6** present the lowest energy on account of the disposition of the thread inside the chiral cavity and the different non-covalent interactions established between the two components of the [2]rotaxanes. The solely presence of one small methyl group at the macrocyclic counterpart of the rotaxane structure, breaking the symmetry of the system, is enough to achieve high levels of enantioselectivities as the chiral information is efficiently transferred through the mechanical bond. Aimed to develop new enantioselective transformations triggered inside the macrocyclic cavity, the design of other chiral polyamide macrocycles is ongoing in our laboratories.

## Acknowledgements

This work was supported by the MICIN/AEI/10.13039/501100011033 (Project PID2020-113686GBI00) and Fundacion Seneca-CARM (Project 20811/PI/18). A. Saura-Sanmartin also thank Fundacion Seneca-CARM for his contract (20259/FPI/17) and Ministerio de Universidades of the Government of Spain for his Margarita Salas postdoctoral

contract (financed by the European Union—NextGenerationEU).

## Conflict of Interest

The authors declare no conflict of interest.

## Data Availability Statement

The data that support the findings of this study are available in the supplementary material of this article.

**Keywords:** Base-Promoted Cyclization · Chirality Transfer Process · Enantioselective · Hydrogen-Bonded Rotaxanes · Mechanostereoisomers

- [1] W. A. Nugent, T. V. RajanBabu, M. J. Burk, *Science* **1993**, 259, 479–483.
- [2] R. S. Cahn, C. Ingold, V. Prelog, *Angew. Chem. Int. Ed. Engl.* **1966**, 5, 385–415; *Angew. Chem.* **1966**, 78, 413–447.
- [3] E. M. G. Jamieson, F. Modicom, S. M. Goldup, *Chem. Soc. Rev.* **2018**, 47, 5266–5311.
- [4] J. R. J. Maynard, S. M. Goldup, *Chem* **2020**, 6, 1914–1932.
- [5] a) A. Martinez-Cueva, A. Saura-Sanmartin, M. Alajarin, J. Berna, *ACS Catal.* **2020**, 10, 7719–7733; b) A. W. Heard, J. Meijide Suárez, S. M. Goldup, *Nat. Chem. Rev.* **2022**, 6, 182–196; c) C. Kwamen, J. Niemeyer, *Chem. Eur. J.* **2021**, 27, 175–186.
- [6] N. Pairault, J. Niemeyer, *Synlett* **2018**, 29, 689–698.
- [7] J. Y. C. Lim, I. Marques, V. Felix, P. D. Beer, *J. Am. Chem. Soc.* **2017**, 139, 12228–12239.
- [8] C. J. Bruns, J. F. Stoddart, *The Nature of the Mechanical Bond: From Molecules to Machines*, Wiley-VCH, Weinheim, **2016**.
- [9] Y. Cakmak, S. Erbas-Cakmak, D. A. Leigh, *J. Am. Chem. Soc.* **2016**, 138, 1749–1751.
- [10] C. Yamamoto, Y. Okamoto, T. Schmidt, R. Jager, F. Vogtle, *J. Am. Chem. Soc.* **1997**, 119, 10547–10548.
- [11] A. W. Heard, S. M. Goldup, *Chem* **2020**, 6, 994–1006.
- [12] C. Tian, S. Fielden, B. Pérez-Saavedra, I. J. Vitorica-Yrezabal, D. A. Leigh, *J. Am. Chem. Soc.* **2020**, 142, 9803–9808.
- [13] K. Nakazono, T. Takata, *Symmetry* **2020**, 12, 144.
- [14] R. Isnin, A. E. Kaifer, *J. Am. Chem. Soc.* **1991**, 113, 8188–8190.
- [15] M. R. Craig, M. G. Hutchings, T. D. W. Claridge, H. L. Anderson, *Angew. Chem. Int. Ed.* **2001**, 40, 1071–1074; *Angew. Chem.* **2001**, 113, 1105–1108.
- [16] W. P. Joon, J. S. Hyun, *Org. Lett.* **2004**, 6, 4869–4872.
- [17] T. Oshikiri, Y. Takashima, H. Yamaguchi, A. Harada, *J. Am. Chem. Soc.* **2005**, 127, 12186–12187.
- [18] Q. C. Wang, X. Ma, D. H. Qu, H. Tian, *Chem. Eur. J.* **2006**, 12, 1088–1096.
- [19] T. Oshikiri, Y. Takashima, H. Yamaguchi, A. Harada, *Chem. Eur. J.* **2007**, 13, 7091–7098.
- [20] Y. Akae, H. Sogawa, T. Takata, *Angew. Chem. Int. Ed.* **2018**, 57, 14832–14836; *Angew. Chem.* **2018**, 130, 15048–15052.
- [21] C. J. Bruns, *Symmetry* **2019**, 11, 1249.
- [22] G. Li, Z. Wang, R. Lu, Z. Tang, *Tetrahedron Lett.* **2011**, 52, 3097–3101.
- [23] M. A. Reddy, N. Bhanumathi, K. R. Rao, *Chem. Commun.* **2001**, 1974–1975.
- [24] A. Nakamura, Y. Inoue, *J. Am. Chem. Soc.* **2003**, 125, 966–972.
- [25] K. Kanagaraj, K. Pitchumani, *J. Org. Chem.* **2013**, 78, 744–751.

- [26] F. Macaev, V. Boldescu, *Symmetry* **2015**, *7*, 1699–1720.
- [27] M. Krajnc, J. Niemeyer, *Beilstein J. Org. Chem.* **2022**, *18*, 508–523.
- [28] S. Saito, Y. Hirano, Y. Mutoh, T. Kasama, *Chem. Lett.* **2015**, *44*, 1509–1511.
- [29] F. Ishiwari, K. I. Fukasawa, T. Sato, K. Nakazono, Y. Koyama, T. Takata, *Chem. Eur. J.* **2011**, *17*, 12067–12075.
- [30] N. Pairault, H. Zhu, D. Jansen, A. Huber, C. G. Daniliuc, S. Grimme, J. Niemeyer, *Angew. Chem. Int. Ed.* **2020**, *59*, 5102–5107; *Angew. Chem.* **2020**, *132*, 5140–5145.
- [31] Y. Tachibana, N. Kihara, T. Takata, *J. Am. Chem. Soc.* **2004**, *126*, 3438–3439.
- [32] J. Y. C. Lim, I. Marques, V. Félix, P. D. Beer, *Angew. Chem. Int. Ed.* **2018**, *57*, 584–588; *Angew. Chem.* **2018**, *130*, 593–597.
- [33] K. Hirose, Y. Nakamura, Y. Tobe, *Org. Lett.* **2009**, *11*, 145–147.
- [34] Y. Tachibana, N. Kihara, Y. Ohga, T. Takata, *Chem. Lett.* **2000**, *29*, 806–807.
- [35] K. Xu, K. Nakazono, T. Takata, *Tetrahedron Lett.* **2016**, *57*, 4356–4359.
- [36] S. Hoekman, M. O. Kitching, D. A. Leigh, M. Pappmeyer, D. Roke, *J. Am. Chem. Soc.* **2015**, *137*, 7656–7659.
- [37] Y. Makita, N. Kihara, T. Takata, *Synthesis and kinetic resolution of directional isomers of [2]rotaxanes bearing a lariat crown ether wheel*, *Supramolecular Chemistry, Vol. 33*, Taylor and Francis, New York, **2021**, <https://doi.org/10.1080/10610278.2021.1895994>.
- [38] A. Martínez-Cuezva, C. Lopez-Leonardo, D. Bautista, M. Alajarin, J. Berna, *J. Am. Chem. Soc.* **2016**, *138*, 8726–8729.
- [39] A. Martínez-Cuezva, C. Lopez-Leonardo, M. Alajarin, J. Berna, *Synlett* **2019**, *30*, 893–902.
- [40] A. Martínez-Cuezva, A. Pastor, M. Marin-Luna, C. Diaz-Marin, D. Bautista, M. Alajarin, J. Berna, *Chem. Sci.* **2021**, *12*, 747–756.
- [41] A. Martínez-Cuezva, D. Bautista, M. Alajarin, J. Berna, *Angew. Chem. Int. Ed.* **2018**, *57*, 6563–6567; *Angew. Chem.* **2018**, *130*, 6673–6677.
- [42] P. Waelès, M. Gauthier, F. Coutrot, *Angew. Chem. Int. Ed.* **2021**, *60*, 16778–16799; *Angew. Chem.* **2021**, *133*, 16916–16937.
- [43] M. Gauthier, P. Waelès, F. Coutrot, *ChemPlusChem* **2022**, *87*, e2021004.
- [44] J. Tanuwidjaja, H. M. Peltier, J. A. Ellman, *J. Org. Chem.* **2007**, *72*, 626–629.
- [45] D. González Cabrera, B. D. Koivisto, D. A. Leigh, *Chem. Commun.* **2007**, 4218–4220.
- [46] R. J. Bordoli, S. M. Goldup, *J. Am. Chem. Soc.* **2014**, *136*, 4817–4820.
- [47] Deposition Numbers 2174455 [for (*R,S*<sub>mp</sub>)-**9a**] and 2174448 [for (*R*)-**21**] contain the supplementary crystallographic data for this paper. These data are provided free of charge by the joint Cambridge Crystallographic Data Centre and Fachinformationszentrum Karlsruhe Access Structures service.
- [48] J. Berná, M. Alajarin, J. S. Martínez-Espín, L. Buriol, M. A. P. Martins, R. A. Orenes, *Chem. Commun.* **2012**, *48*, 5677–5679.
- [49] C. Lopez-Leonardo, A. Martínez-Cuezva, D. Bautista, M. Alajarin, J. Berna, *Chem. Commun.* **2019**, *55*, 6787–6790.
- [50] A. Martínez-Cuezva, F. Morales, G. R. Marley, A. Lopez-Lopez, J. C. Martínez-Costa, D. Bautista, M. Alajarin, J. Berna, *Eur. J. Org. Chem.* **2019**, 3480–3488.
- [51] A. Martínez-Cuezva, L. V. Rodrigues, C. Navarro, F. Carro-Guillen, L. Buriol, C. P. Frizzo, M. A. P. Martins, M. Alajarin, J. Berna, *J. Org. Chem.* **2015**, *80*, 10049–10059.
- [52] Aimed to study a potential epimerization process through a deslipping-slipping process, we monitored a solution of **9a** in DMF-*d*<sub>7</sub> at 25 °C, only observing a slow dethreading which was accelerated at higher temperatures (Figure S2).
- [53] A. Saura-Sanmartin, A. Martínez-Cuezva, A. Pastor, D. Bautista, J. Berna, *Org. Biomol. Chem.* **2018**, *16*, 6980–6987.
- [54] A. Basak, S. C. Ghosh, *Synlett* **2004**, 1637–1639.
- [55] For the synthesis of *rac-trans*- $\gamma$ -lactam **23e**, see: S. W. Laws, S. Y. Howard, R. Mato, S. Meng, J. C. Fettinger, J. T. Shaw, *Org. Lett.* **2019**, *21*, 5073–5077.
- [56] For the synthesis of *rac-trans*- $\gamma$ -lactam **24a**, see: M. Pohmakotr, N. Yotapan, P. Tuchinda, C. Kuhakarn, V. Reutrakul, *J. Org. Chem.* **2007**, *72*, 5016–5019.
- [57] M. Park, S. M. Kim, K. Choi, *Org. Biomol. Chem.* **2012**, *10*, 8051–8054.
- [58] T. J. Seguin, T. Lu, S. E. Wheeler, *Org. Lett.* **2015**, *17*, 3066–3069.
- [59] T. J. Seguin, S. E. Wheeler, *Angew. Chem. Int. Ed.* **2016**, *55*, 15889–15893; *Angew. Chem.* **2016**, *128*, 16121–16125.
- [60] C. J. Laconsay, T. J. Seguin, S. E. Wheeler, *ACS Catal.* **2020**, *10*, 12292–12299.

Manuscript received: July 6, 2022

Accepted manuscript online: August 2, 2022

Version of record online: August 19, 2022